Neurochemical Research (2022) 47:1904–1916
https://doi.org/10.1007/s11064-022-03574-4

ORIGINAL PAPER

Liraglutide Ameliorates Cerebral Ischemia in Mice via Antipyroptotic Pathways

Lan Yang[1,2] · Junmin Cheng[1,2] · Guang Shi[1,2] · Cong Zhang[1,2] · Yuanyuan Du[1,2] · Linyu Chen[1,2] · Huimin Qiao[1,2] · Rong Chen[1,2] · Xiangjian Zhang[1,2]

Received: 25 November 2021 / Revised: 3 March 2022 / Accepted: 8 March 2022 / Published online: 29 March 2022

Abstract

It was recently shown that pyroptosis, an inflammatory form of programmed cell death, is critically involved in the pathogenesis of ischemic stroke. Liraglutide (Lg) is a novel long-acting analog of glucagon-like peptide-1 that has potential protective effects against stroke. However, the relationship between Lg and pyroptosis in the brain is not well defined. In this study, we found that injection of Lg significantly improved the recovery of motor function, increased cerebral blood flow and ameliorated cerebral damage in a mouse model of focal cerebral cortical ischemia. Our results revealed that Lg treatment significantly reduced the levels of NLRP3, Caspase1, IL-1β and the pore-forming protein gasdermin D in microglial cells in vitro, suggesting that the neuroprotective effect of Lg may be achieved through the inhibition of pyroptosis. Furthermore, by using a specific inhibitor of NOD-like receptor protein 3 (NLRP3), we confirmed that the antipyroptotic mechanism of Lg may be mediated by NLRP3 in vivo. Our present study unveils a novel neuroprotective mechanism through which Lg alleviates ischemia by exerting NLRP3-dependent antipyroptotic effects.

Keywords Liraglutide (Lg) · Pyroptosis · NOD-like receptor protein 3 (NLRP3) · Cerebral ischemia

Introduction

Ischemic stroke is one of the leading causes of disability and mortality worldwide and imposes severe social and economic burdens [1, 2]. Intravenous thrombolysis and endovascular intervention are only applied in a small number of patients due to strict indications for treatment, limited therapeutic availability and uncontrollable side effects [3, 4]. Therefore, new targeted therapies and exploration of their effects on ischemic stroke recovery are urgently needed.

Distinct from apoptosis and necrosis, pyroptosis is a recently discovered form of programmed cell death that is closely associated with the inflammatory response [5, 6]. Pyroptosis is activated by the cleavage of Caspase1, which can be triggered by the NOD-like receptor protein 3 (NLRP3) inflammasome, and conversion of inactive IL-1β and IL-18 into their active forms by activated Caspase1. The process of pyroptosis is often accompanied by the release of a variety of proinflammatory factors [7, 8].

Liraglutide (Lg) is a novel long-acting analog of glucagon-like peptide 1 (GLP-1) that can stimulate glucose-dependent insulin secretion from pancreatic beta cells and inhibit the secretion of glucagon REF. It is widely used for the treatment of type 2 diabetes mellitus and rarely causes hypoglycemia REF. Lg is able to penetrate the blood–brain barrier in rodents, and GLP-1 receptor (GLP-1R) is expressed not only in the pancreas but also in the brain, suggesting that it may play an important role in the central nervous system [9, 10]. A study [11] demonstrated that Lg can dose-dependently limit the infarct size. Indeed, Lg has been shown to exert protective effects against cerebral ischemia reperfusion injury in mice [12, 13]. Moreover, a recent study demonstrated that Lg ameliorates nonalcoholic steatohepatitis by inhibiting the activation of the NLRP3 inflammasome and pyroptosis [14]. However, whether Lg also has a similar effect in cerebral ischemia has not yet been reported. Based on these findings, in the present study, we

✉ Xiangjian Zhang
zhang6xj@aliyun.com

[1] Department of Neurology, Second Hospital of Hebei Medical University, 215 Hepingxi Road, Shijiazhuang 050000, Hebei, China

[2] Hebei Key Laboratory of Vascular Homeostasis and Hebei Collaborative Innovation Center for Cardio-Cerebrovascular Disease, 215 Hepingxi Road, Shijiazhuang, Hebei, China

aimed to elucidate whether Lg has neuroprotective functions in a mouse model of focal cerebral cortical ischemia and to investigate the underlying mechanisms.

Materials and Methods

Animals and Stroke Model

Adult male C57BL/6 mice (3-month old, weighing 23–29 g) were purchased from Vital River Laboratory Animal Technology (Beijing, China). The mice were individually housed under temperature-controlled conditions (humidity: 60 ± 5%; temperature: 22 ± 3 °C) with free access to diet and water under a 12 h light/12 h dark cycle. After 3 days of adaptation to the surrounding environment, the animals were subjected to the following procedures. The animal care and experiments protocols were approved by the Animal Care and Management Committee of Second Hospital of Hebei Medical University and performed in accordance with the ARRIVE Guidelines for the Care and Use of Laboratory Animals [15].

Male C57BL/6 mice underwent distal middle cerebral artery occlusion (dMCAO) as previously described [16, 17]. In brief, the mice were anesthetized with avertin (400 mg/kg, Sigma–Aldrich). The right common carotid was exposed and permanently ligated with silk surgical sutures. The right middle cerebral artery (MCA) was then revealed, and the distal branch of the MCA was perpetually coagulated with a cauterizer (Bovie, USA) without damaging the brain surface. Mice in the sham-operated group were subjected to the same operation described above without occlusion and/or coagulation. During dMCAO, the body temperature of the mice was maintained at 37.5 ± 0.5 °C.

Experimental Designs and Treatment

The detailed experimental protocols are shown in Fig. 1. The aim of this study was to assess the efficacy of Lg in an animal model of ischemic stroke. The mice were randomly divided into three groups: the sham group, dMCAO group, and dMCAO + Lg group. The dMCAO + Lg group received subcutaneous injection of Lg (246.7 μg/kg/day), which was dissolved in 0.9% saline, for 3 consecutive days before and after surgery [18, 19]. At the end of the experiment, the mice were sacrificed by rapid decapitation under deep anesthesia, and samples were collected for further analyses.

Measurement of Body Weight and Blood Glucose Levels

Peripheral blood was collected before dMCAO and on days 1, 2 and 3 after dMCAO, and the body weight of the mice was measured at the same times. The blood glucose level was measured with a glucometer (Roche Diagnostics, Mannheim, Germany) according to the manufacturer's instructions.

Behavioral Testing

Neurological Scores

The modified Neurological Severity Score (mNSS) was used to assess motor function, sensory function, reflexes, and balance on a scale of 0–18 (normal score: 0; maximal deficits: 18) as described previously [20, 21]. Higher scores indicated more severe neurological deficits.

The Rotarod Test

The rotarod test was used to assess the motor function of mice as described previously [22]. Before the test, all mice were subjected to training trials three times per for 5 days over a 15-min period. The test was then conducted for 3 days after surgery. During the test, mice were placed on a rotating Rota-Rod cylinder that accelerated from 4 to 40 rpm for no more than 300 s. The mean values were used for statistical analysis.

Gait Analysis

The mice were analyzed using a TreadScan instrument (Columbus Instruments, Columbus, OH) according to the manufacturer's instructions [23]. The video treadmill system consisted of a treadmill belt and a mirror mounted underneath. A high-speed digital video camera was installed under the treadmill to record the movements of the four paws at 100 frames per second for 20 s. A background image was obtained before each test. Each mouse was trained 3 days prior to dMCAO, and the test was performed at a speed of 8 cm/s for 3 days after surgery. Six consecutive step cycles were selected for automatic gait analysis, and the values for each limb were analyzed with CleverSys TreadScan software (CleverSys, Inc., Reston, VA).

Assessment of Brain Infarct Volume

The brain infarct volume was assessed on day 3 and day 7 after dMCAO by 2,3,5-triphenyltetrazolium chloride (TTC) staining. The brains of the mice (n = 6) were dissected, and the brain tissues were sectioned into eight slices of 1 mm thickness, stained with 2% TTC solution at 37 °C for 15 min and then fixed with 4% paraformaldehyde (PFA). Normal brain tissue appeared red, while the infarct area appeared pale. The infarct volume was measured by ImageJ software. The infarct volume was calculated as %HLV = {[total infarct

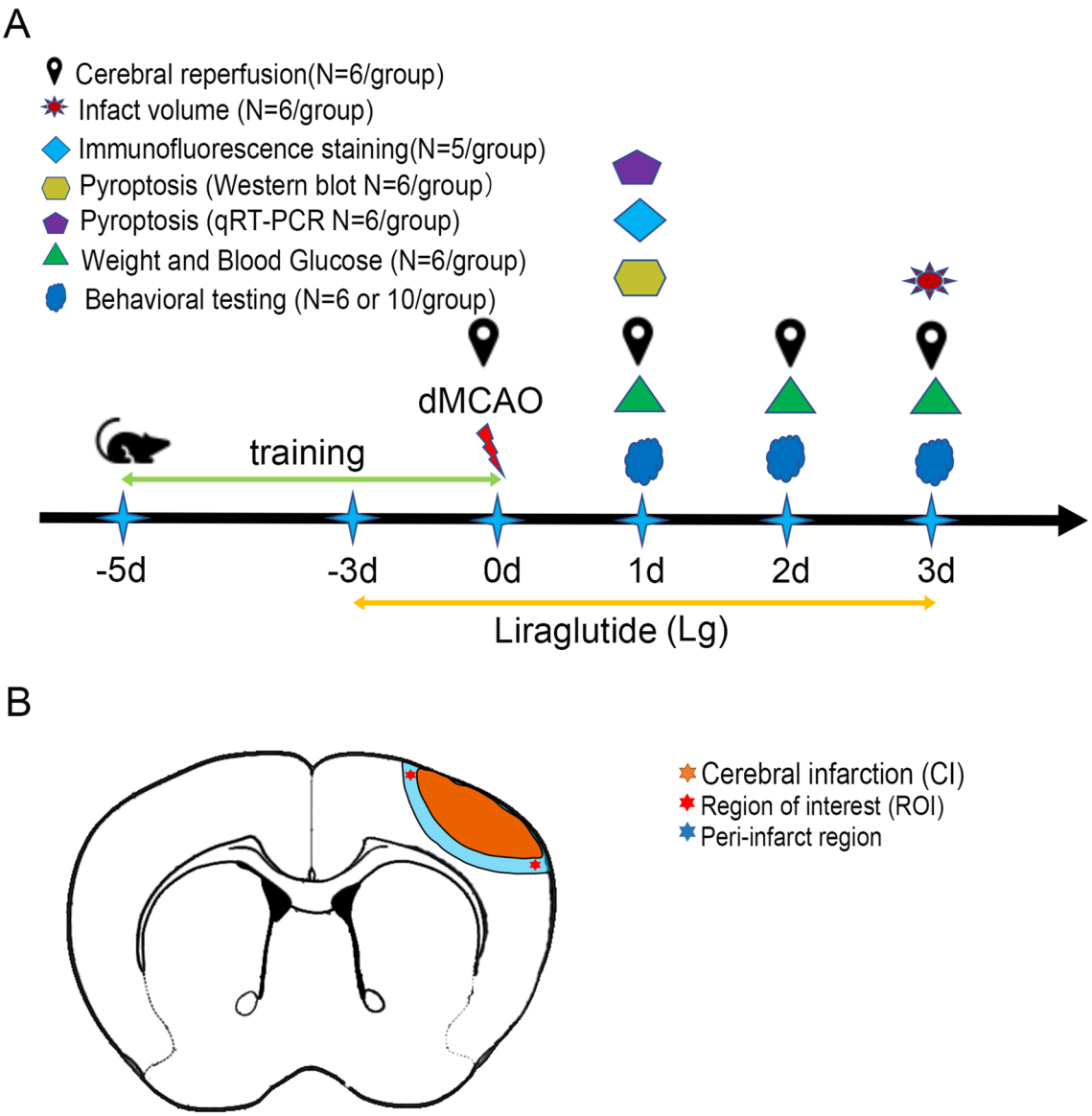

Fig. 1 Experimental outline and schematic diagram of brain section. **A** Experimental outline: liraglutide was administrated intraperitoneally 3 days before surgery, once daily, and then until 3 days after stroke. Neurobehavioral tests were performed at days 1, 2, and 3 after stroke. Pyroptosis was evaluate at the indicated time points. The number of mice in each group for each test are shown in parentheses. **B** Schematic diagram of brain section. Red star indicates the region of interest in the ipsilateral peri-infarct cortex, in which immunofluorescence images were collected. Blue strip (0.5 mm wide) indicates peri-infarct region, in which brain samples were harvested for qRT-PCR and western blot

volume—(volume of the intact ipsilateral hemisphere—volume of the intact contralateral hemisphere)]/contralateral hemisphere volume}.

Monitoring of Cerebral Blood Flow (CBF)

A real-time laser speckle blood flow imager (PeriCam PSI System, Perimed, Sweden) was used to monitor the change in cerebral blood flow at different times before and after dMCAO (n = 6). After successful intravenous anesthesia with tribromoethanol, the skull was fully exposed, the periosteum was carefully separated and fixed on a stereotaxic device, and CBF was measured. PimSoft 1.3 (Perimed AB, Sweden) was used to calculate the mean perfusion level of the region of interest (ROI), including changes in CBF from the right cortical infarct area to both hemispheres. The experimental procedures were completed in a sterile environment, and the body temperature of the mice was maintained at 37 ± 0.2 °C.

Immunofluorescence Staining

Deeply anesthetized mice were intracardially perfused with cold phosphate–buffered saline (PBS), followed by 4% PFA. Frozen coronal brain sections were processed for immunohistochemical staining as previously described [24]. The sections (15 μm) were permeabilized with 0.3% Triton X-100 for 15 min, blocked with 10% normal donkey serum for 1 h at 37 °C, and incubated with primary antibodies overnight at 4 °C. The primary antibodies included a rabbit anti-NLRP3 antibody (1:300, Bioworld Technology); goat anti-Iba-1 antibody (1:500, Abcam); rabbit anti-Caspase1 antibody (1:200, ABclonal); and rabbit anti-IL-1β antibody (1:100, Abcam). The next day, the samples were washed with PBS and incubated with secondary antibodies (Alexa Fluor 488- or 594-conjugated, Jackson ImmunoResearch, USA) at 37 °C for 2 h. Images were acquired with a Laser Scanning Confocal Microscope (Zeiss, LSM880, Germany). Three-dimensional (3D) images were processed using Imaris software (Bitplane, RRID:SCR_007370). The number of positive cells in 5 different fields of the peri-infarct area in the cortex (n = 6 per group) was determined and analyzed with ImageJ software.

Quantitative Real-Time Polymerase Chain Reaction (PCR)

At 24 h after dMCAO, brain tissues were obtained from the peri-infarct region and the corresponding region in the sham group (n = 6). Total RNA was extracted, and quantitative real-time PCR was performed as previously described [25]. The primer sequences are listed in Table 1.

Western Blotting

As previously described [26], proteins were extracted from the peri-infarct region of the cortex (n = 6) at 4 °C using radioimmunoprecipitation assay (RIPA) buffer (Solarbio) containing 1% protease inhibitor cocktail (Sigma Cat# P8340) and 1% phosphatase inhibitor (Applygen Cat# P1260). The protein concentration was determined using a BCA Protein Assay reagent kit (Novagen, Madison, WI, USA). Equal amounts (50 μg) of protein samples were separated by 10% SDS–PAGE and transferred onto a polyvinylidene difluoride (PVDF) membrane (Roche, USA), which was blocked with fast sugar-free blocking solution for 1 h. The membrane was then incubated with an anti-NLRP3 (1:1000, Bioworld Technology), anti-Pro Caspase1 (1:1000, Proteintech), anti-Cleaved Caspase1 P10 (1:1000, Proteintech), anti-Gsdmd (1:1000, Arigo), anti-Asc (1:1000, SAB), anti-Pro IL-1β (1:1000, Bioworld Technology), or anti-Cleaved IL-1β (1:5000, Abcam) primary antibody overnight at 4 °C. The next day, the membrane was washed three times with TBST and incubated with DyLight 800-conjugated goat anti-rabbit IgG (H&L) secondary antibody (1:10,000, Rockland) for 1 h at room temperature. Images were obtained with an Odyssey infrared scanner (LICOR Bioscience, USA). GAPDH (1:20,000, Bioworld Technology) was used as a loading control.

Cell Culture and Treatment

Mouse microglial cells (BV2 cells, 1101MOUPUMC00063) were purchased from the National Biomedical Laboratory Cell Resource Bank of China. The BV2 cells were cultured in high-glucose Dulbecco's modified Eagle's medium (DMEM) containing 4 mM L-glutamine, 4500 mg/L glucose (HyCloneTM; GE Healthcare Life Sciences, South Logan, UT, USA), 10% fetal bovine serum and a 1% penicillin mixture (Solarbio, China) at 37° in an incubator containing 5% CO_2. The cells were used for experiments when the confluency reached 80–90%. To mimic ischemic stroke conditions, BV2 cells were subjected to oxygen–glucose deprivation (OGD) as described previously [27]. The cells in the OGD group were cultured with glucose-free medium (Gibco, USA) and kept in a hypoxic incubator chamber containing premixed gas (94% N_2, 1% O_2 and 5% CO_2) at 37 °C. Mcc950 (MedChemExpress, 20 μM), a specific inhibitor of NLRP3, was applied for 30 min before other treatments. To confirm the effect of the drug, the cells were divided into the control group, OGD group, and OGD + Lg groups (10–1000 μM Lg). In subsequent experiments, the cells were divided into the control group, OGD group, OGD + Lg group (200 μM Lg), and OGD + Mcc950 group.

Cell Viability Assay

A cell counting kit-8 (CCK-8, Dojindo, Japan) was used to determine the viability of BV2 cells subjected to OGD. BV2

Table 1 Primers for RT-qPCR

Primers	Forward (5′–3′)	Reverse (5′–3′)
$NLRP_3$	CCAGCCAGAGTGGAATGACA	AGCGGGAGACAAATGGAGAT
Caspase-1	GGGACCCTCAAGTTTTGCC	GACGTGTACGAGTGGTTGTATT
ASC	AAGAGTCTGGAGCTGTGGCA	CTGTGACCCTGGCAATGAGT
IL-1β	AACTCAACTGTGAAATGCCACC	CATCAGGACAGCCCAGGTC
Gsdmd	CGAGTGGCCCAACTGCTTAT	ATGGAACAAAGCGCAGCAAG

cells were seeded in 96-well plates at a density of 2×10^5 cells/ml. After OGD, 10 µl of CCK-8 reagent was added to each well of the 96-well plates followed by incubation at 37 °C for 2 h. The reaction was evaluated by measuring the absorbance at 450 nm. Five replicate wells were set up for each group, and the results shown are representative of 3 independent experiments.

Enzyme-Linked Immunosorbent Assay (ELISA)

The supernatants of cultured cells were collected after OGD. IL-1β and IL-18 concentrations were measured with mouse IL-1β and IL-18 ELISA kits (Multi Sciences EK201B and EK218) according to the manufacturer's instructions. Three independent experiments were performed.

Statistical Analyses

All data were analyzed with GraphPad Prism 8.0 software (GraphPad Software, San Diego, CA, USA). The data were first tested for normality, and Levene's test was performed to assess the uniformity of the variance. Quantitative data are expressed as the mean ± S.D. If normally distributed, the data are expressed as the median and interquartile range. One-way analysis of variance (ANOVA) followed by Tukey's multiple comparison test was used for comparisons among multiple groups. Nonparametric analyses of mNSS were performed with the Kruskal–Wallis test. Student's t test was employed to compare the TTC-positive area between two groups. $P < 0.05$ was considered statistically significant.

Results

Lg Reduces the Infarct Volume After dMCAO

The GLP-1R agonist Lg is a long-acting hypoglycemic drug that reduces blood sugar levels and body weight in diabetic patients over the long term. Since blood sugar levels can affect the prognosis of cerebral infarction [28], we first evaluated whether short-term application of Lg affects blood glucose levels. The results indicated that there was no significant difference in blood glucose levels or body weight between the Lg-treated and untreated dMCAO groups ($p > 0.5$, 7.73 ± 0.47 mmol/L versus 7.42 ± 0.45 mmol/L on day 1; Fig. 2A and B), consistent with previous studies [29, 30]. TTC staining was used to measure the infarct volume in the different groups at day 3 and day 7 after dMCAO to analyze neurons. Compared with the untreated dMCAO group, the Lg-treated dMCAO group exhibited a significant reduction in the infarct volume ($p = 0.0061$ on day 3; Supplementary Figs. 1A, B and 2 C, D). Together, these results suggest that Lg is safe, limits pathological progression after dMCAO and may therefore constrain the infarct volume after dMCAO.

Lg Improves Neurological Recovery

We then assessed mNSSs and conducted the rotarod test and gait analysis on consecutive days after dMCAO to evaluate neurological function recovery. Neurological function was dramatically impaired in both Lg-treated and untreated dMCAO animals compared to sham-operated animals (Fig. 3A). However, there was a significant improvement in the Lg-treated group ($p < 0.05$, $n = 10$), which displayed greater restoration of neurological function (Fig. 3A). Compared with no treatment, Lg significantly improved the performance of dMCAO animals in the rotarod test (Fig. 3B; $p = 0.0128$, $n = 10$). In addition, limb function was substantially restored in the Lg-treated mice (Fig. 3C–F). Compared to that of the untreated dMCAO animals, the instantaneous running speed of the mice in the Lg-treated dMCAO group increased continuously over 3 days, with the increase being particularly pronounced on day 3 ($p = 0.0039$, $n = 6$). The mice in the Lg-treated group had a shorter stride length (Lg-treated group: 58.80 ± 5.17 mm versus untreated dMCAO group: 67.26 ± 4.54 mm on day 3; $p = 0.0130$, $n = 6$), smaller average print area (Lg-treated group:17.02 ± 1.87 mm^2 versus control untreated group: 20.08 ± 1.88 mm^2 at day 3; $p = 0.0178$, $n = 6$) and improved LF-Gait angles ($p = 0.0497$, $n = 6$) on day 3. All results reveal that Lg treatment significantly improves the motor function of C57BL/6 mice subjected to dMCAO.

Lg Increases Cerebral Perfusion After Focal Cerebral Infarction

A laser speckle instrument was used to monitor the changes in CBF on the lesion side in dMCAO mice at different time points. On day 3 after the surgery, CBF on the lesion side was significantly increased in the Lg-treated group ($p = 0.0191$), whereas there was no improvement in the untreated group (Fig. 4A, B), consistent with our previous findings [29, 31]. These results demonstrate that Lg may promote angiogenesis after focal cerebral ischemia in mice.

Lg Inhibits Pyroptosis in the Peri-infarct Cortex After Stroke

To evaluate the potential relationship between Lg treatment and pyroptosis, we first determined the mRNA expression of pyroptosis-related genes on day 1 after surgery. The results revealed that the mRNA expression of NLRP3, IL-1β, Caspase1 and Gsdmd was upregulated in dMCAO mice compared with sham-operated mice ($p = 0.0002$, 0.0008, 0.0182, and 0.0108, respectively; Fig. 5B) and that administration of

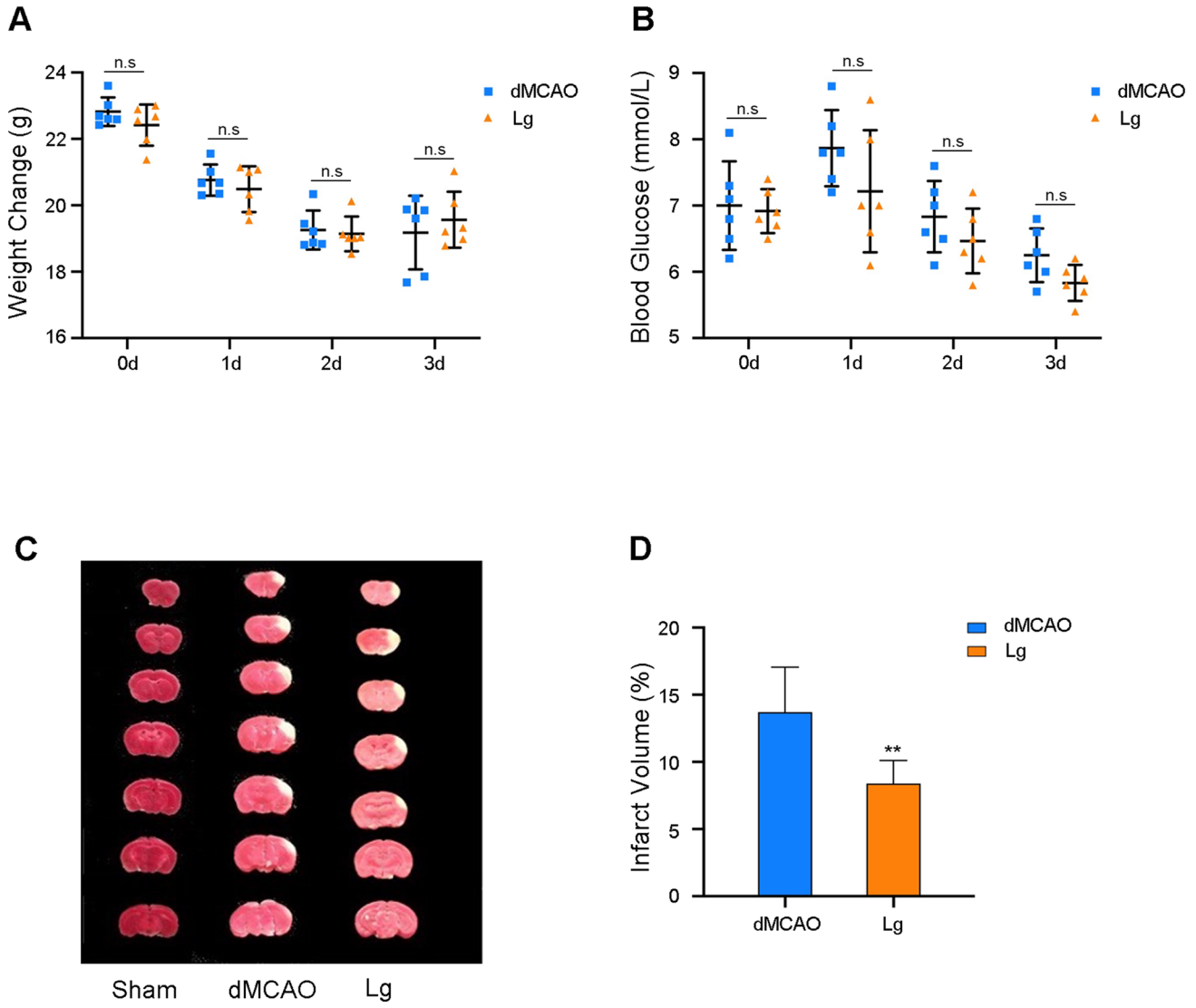

Fig. 2 Liraglutide ameliorates infarct volume after dMCAO. Results for **A** animal body weight; **B** blood glucose level; **C** representative TTC-stained images in Lg-treated and control-treated dMCAO mice at day 3 after stroke; **D** quantification of the infarct volume. Data in **A**–**C** (n = 6) are expressed as mean ± SD. Graph bar in **A**, **B**, and **D** are based on unpaired two-tailed Student's t-test. *n.s* no statistical difference. $*p < 0.05$, $**p < 0.01$

Lg induced a downward trend in the mRNA levels of these molecules (p = 0.0019, 0.0006, 0.0284 and 0.0346, respectively; Fig. 5B). The changes in protein expression levels were consistent with the changes in gene expression. As shown in Fig. 5A, C and D, the protein levels of NLRP3, Pro IL-1β, Cleaved IL-1β, Caspase-1, Cleaved Caspase1 (p10) and Gsdmd were all reduced by Lg treatment (p = 0.0006, 0.0228, 0.0045, 0.0016, 0.0044, and 0.0346, respectively; indicated by the arrowheads). However, we did not observe a significant difference in the gene or protein expression of Asc following Lg treatment (Fig. 5A–D), suggesting that the effect of Lg in alleviating pyroptosis may not be mediated by alterations in Asc abundance after stroke. Lg also significantly reduced the secretion of IL-1β and IL-18 by microglial cells subjected to OGD in vitro (Supplementary Fig. 2). In addition, immunohistochemical analysis of the brain tissues showed that the numbers of cells positive for NLRP3 (red), IL-1β (red), and Caspase1 (red) were markedly reduced in the Lg-treated dMCAO group compared to the untreated dMCAO group (p = 0.0110 for NLRP3; p = 0.0041 for IL-1β; p = 0.0414 for Caspase1; Fig. 5E–G). As shown in Fig. 5, staining for NeuN (green) demonstrated that Lg alleviated pyroptosis after cerebral ischemia. Taken together, these data suggest that Lg is capable of inhibiting pyroptosis in the peri-infarct cortex after stroke.

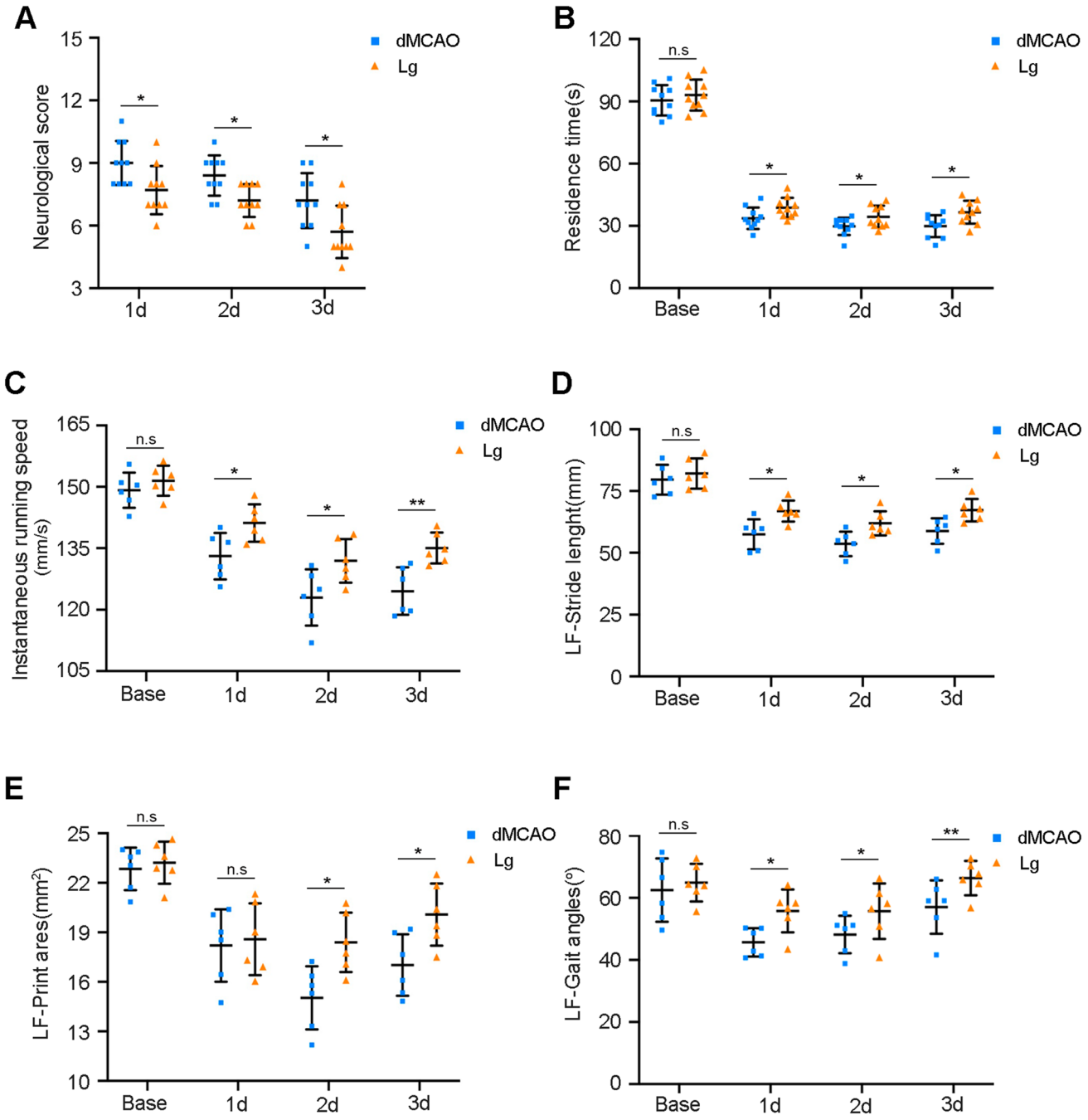

Fig. 3 Liraglutide improves neurological recovery. Results of the **A** neurological deficits scores; **B** rotarod test-residence time; **C** instantaneous running speed test; **D** the stride length for the left limb test; **E** the LF-Print area test; **F** the LF-Gait angles test. Data of **A**, **B** (n = 10) are expressed as mean ± SD, Data of **C**–**F** (n = 6) are expressed as mean ± SD. Statistical significance was assessed by unpaired two-tailed Student's t-test. *n.s* no statistical difference. $*p < 0.05$, $**p < 0.01$

Lg Exerts an Antipyroptosis Effect by Inhibiting the NLRP3/Caspase1/IL-1β Pathway In Vitro

We further investigated the potential mechanism by which Lg prevents pyroptosis in microglial cells after OGD. We first subjected BV2 cells to OGD for various durations (0–12 h) to determine the optimal duration of OGD. OGD treatment for 6 h led to approximately 50% cell death, so this time period was selected for the following experiments (Fig. 6A). The protein expression of NLRP3, Pro IL-1β, Cleaved IL-1β, Pro Caspase1, and Cleaved Caspase1 (p10) was upregulated in microglial cells exposed to OGD, and Lg

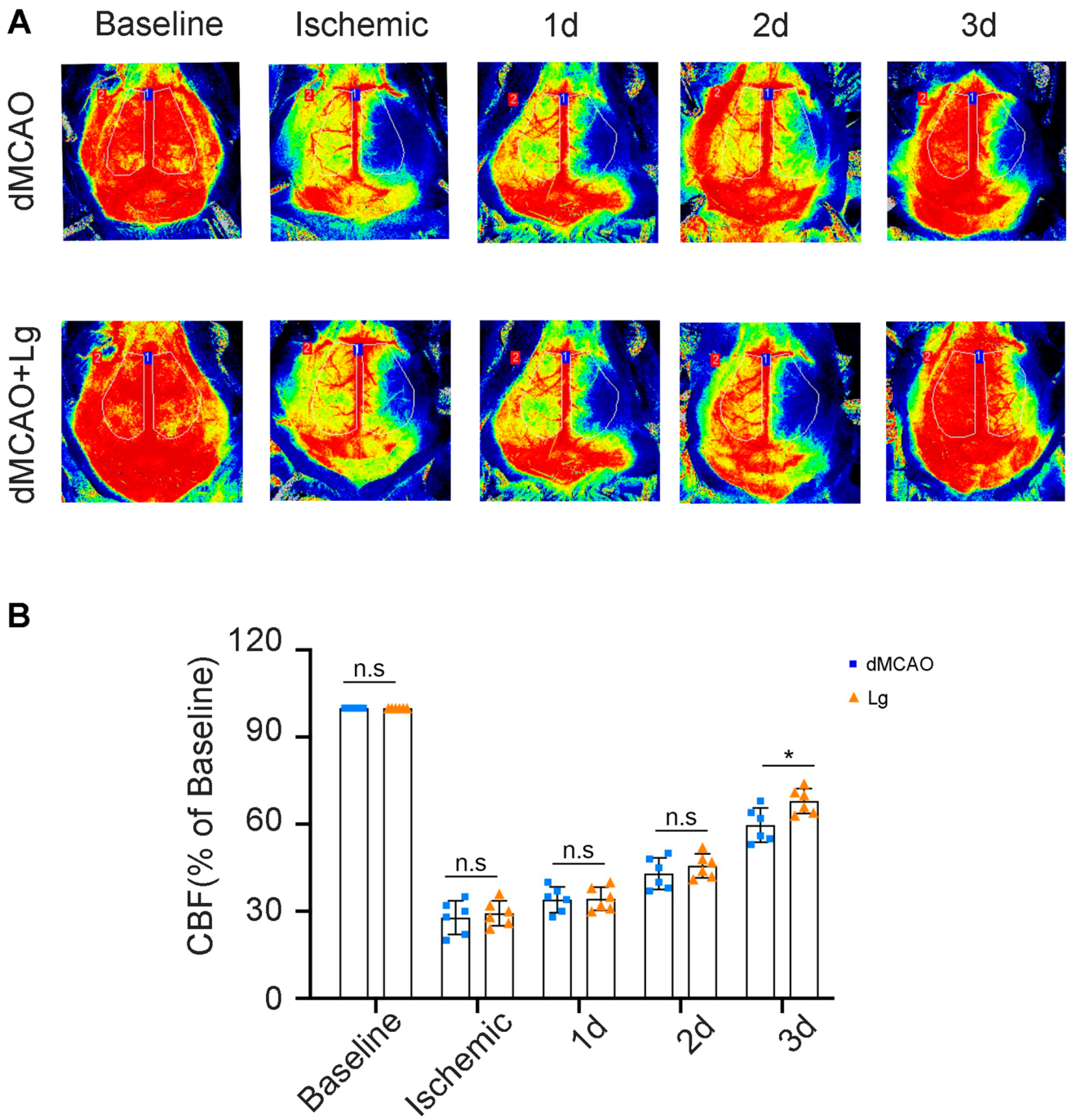

Fig. 4 Liraglutide increases cerebral perfusion in mice with focal cerebral infarction. **A** representative images of Liraglutide treatment on the cerebral blood flow with 2-dimensional laser speckle imaging at indicated time points. **B** quantification of the ipsilateral CBF in dMCAO mice in control and Lg treated groups. Data are expressed as mean ± SD (n = 6); statistical significance was assessed by unpaired two-tailed Student's t-test. *n.s* no statistical difference. *p < 0.05

treatment significantly reduced the expression levels of these proteins (****p < 0.0001; Fig. 6C–G).

We employed Mcc950, a potent and specific small-molecule inhibitor of NLRP3, to further investigate the molecular mechanism underlying the effect of Lg. Compared with the OGD, treatment with Mcc950 decreased the protein levels of NLRP3, Pro Caspase1, Cleaved Caspase1 (p10), IL-1β, and Cleaved IL-1β in BV2 cells, indicating that Mcc950 effectively suppressed the expression of the key molecules involved in pyroptosis (p = 0.0186, 0.0307, 0.0142, 0.0035, and 0.0027, respectively; Fig. 6C–G).

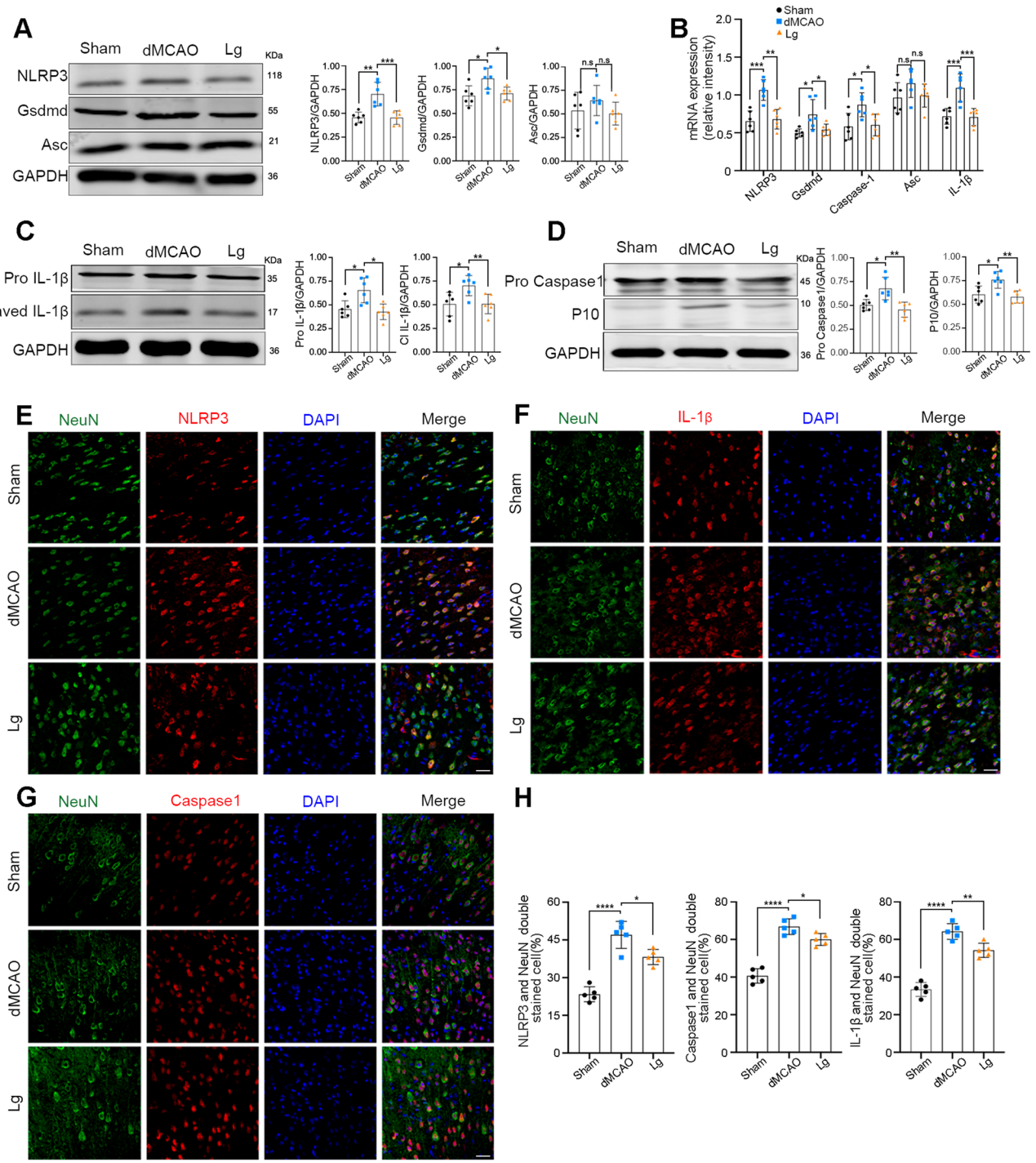

Fig. 5 Liraglutide inhibits pyroptosis in peri-infarct cortex after stroke. **A**, **C**, **D** Western blot and protein quantification analysis of the pyroptosis in peri-infarct cortex at day 1 in C57BL/6 mice after stroke; **B** mRNA expression of NLRP3, Gsdmd, Caspase-1, Asc, IL-1β in peri-infarct cortex at day 1 after stroke; **G** immunofluorescence labeling of NLRP3, ASC and IL-1β (red) and NeuN-positive (green) in Sham group, dMCAO control and dMCAO + Lg treated mice at day 1 after dMCAO. (**Scale bar, 20 μm**). **H** quantitative analysis of NLRP3, ASC and IL-1β-positive puncta. Data of **A**–**D** (n = 6) are expressed as mean ± SD, Data of **E**–**G** (n = 5) are expressed as mean ± SD. Statistical significance was assessed by One-way ANOVA with Tukey's post hoc test. *n.s* no statistical difference. $^{*}p < 0.05$, $^{**}p < 0.01$, $^{***}p < 0.001$

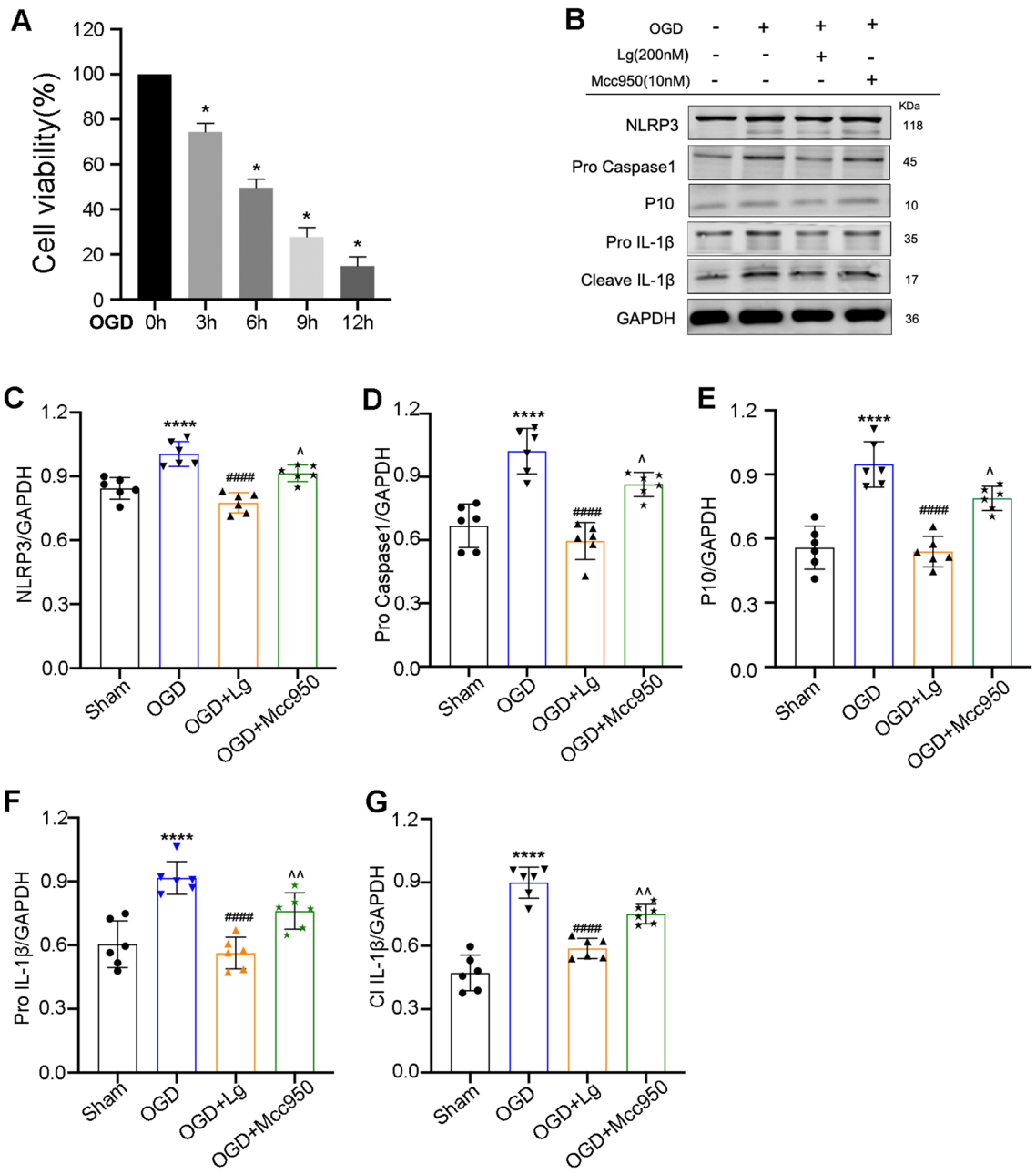

Fig. 6 Liraglutide mediates anti-pyroptosis functions through inhibiting the ARC/ NLRP3/Caspase-1/IL-1β pathway. **A** cell viability of BV2 cells at 0 h, 3 h, 6 h, 9 h, and 12 h after OGD. $^{*}p<0.05$ (n = 5). **B** protein levels of NLRP3, Caspase-1, cleaved-Caspase-1(p10), IL-1β, cleaved- IL-1β in Sham, OGD, OGD + Lg, and OGD + Mcc950. **C–G** quantification of NLRP3, Pro Caspase-1, p10, Pro IL-1β, cleaved IL-1β gene expression in vitro. $^{****}p<0.0001$ (OGD group vs. Sham group), $^{\#\#\#\#}P<0.0001$ (OGD + Lg group vs. OGD group), $^{\wedge}P<0.05$ or $^{\wedge\wedge}P<0.01$ (OGD + Mcc950 group vs. OGD group)

Discussion

In the present study, we employed both in vivo and in vitro models to identify a novel effect of Lg on pyroptosis after cerebral ischemia. Our data demonstrate that Lg treatment significantly reduced the brain infarct volume, improved motor function recovery and exerted anti-inflammatory effects in a mouse model of focal cerebral cortical ischemia. This neuroprotective effect of Lg may be achieved by the inhibition of the NLRP3 inflammasome. To the best of our knowledge, this is the first study to provide proof of a potential antipyroptosis-mediated role for Lg in stroke.

Lg belongs to a family of human incretin GLP-1 analogs. It can cross the blood–brain barrier [32–34] and is widely

used in the treatment of diabetes, obesity [35], Alzheimer's disease, Parkinson's disease and multiple sclerosis [33, 36–39]. Lg binds to the GLP-1 receptor and stimulates the secretion of insulin to decrease blood glucose levels and rarely causes hypoglycemia [40]. Lg has a large number of functions, including antiapoptotic [41, 42], anti-inflammatory, antioxidative [9, 43], and antitumor [44] effects and the ability to promote vascular regeneration [45], dilate cerebral arterioles [46], and limit harmful increases in the levels of free radicals [47–49]. Considering the many targets of Lg, an increasing number of scholars are focusing on this analog in various cerebrovascular studies [48, 50]. It has been reported that Lg promotes brain repair through Sirt1-mediated improvement of mitochondrial function in stroke [51]. A recent study [52] discussed the potential efficacy of GLP-1 agonists in patients with acute ischemic stroke. Consistent with previous studies, our data confirm that Lg indeed reduces the cerebral infarct volume, promotes the recovery of nerve function in the brain and exerts neuroprotective effects (Figs. 2 and 3).

Pyroptosis, a special form of apoptosis, is a recently discovered mode of cell death associated with inflammation and mediated by inflammasome and Caspase1 activation [53]. A number of studies have explored the mechanisms of pyroptosis in different diseases, for example, the outcomes of ischemic stroke [54], Parkinson's disease, cerebral hemorrhage [55] and other systemic diseases [56, 57] can be better controlled by modulating pyroptosis. It has been recently shown that Lg ameliorates nonalcoholic steatohepatitis by inhibiting the NLRP3 inflammasome and pyroptosis activation via mitophagy. Selective NLRP3 inflammasome inhibitors can preserve cardiac function [58], and similarly, decreasing NLRP3-mediated inflammation protects the brain in mice with intracerebral hemorrhage [59]. However, the effect of Lg on pyroptosis in stroke remains unclear. The present study reveals that Lg treatment may downregulate the expression of pyrolysis-related proteins, especially NLRP3 (Fig. 4), suggesting that the neuroprotective effect of Lg is related to not only pyroptosis but also the NLRP3 protein. NLRP3 is known to play a pivotal role in the activation of Caspase1 and downstream cleavage of IL-1β, leading to pyroptosis [60, 61]. Our results demonstrate that Lg may inhibit the secretion of IL-1β and IL-18 in vitro (Supplementary Fig. 2). To further evaluate the underlying molecular mechanism, we used the administered NLRP3 inhibitor Mcc950 in vitro, and the results (Fig. 6) revealed that NLRP3 is the most plausible target of Lg in exerting antipyroptotic effects in cerebral ischemia.

The present study has several limitations. First, we focused only on the effect of Lg in adult male ischemic stroke model mice without other complications. This disregards the prominent role of diabetes mellitus in middle cerebral artery cortical infarction [62, 63], as well as the potential effects in elderly patients and female patients. Further work is needed to address whether our findings related to Lg can be replicated in these settings. Second, all nerve cells, including neurons and microglia, can undergo pyroptosis. In this study, we only investigated the potential mechanism by which Lg inhibits pyroptosis of microglia; however, it is reasonable to assume that Lg has similar effects on pyroptosis in neurons. Further work will be conducted to assess the effect of Lg on neurons.

In summary, our study reveals that Lg has protective effects against pyroptosis in vitro as well as in vivo in the brain following stroke. The primary target of its antipyroptotic effect is the NLRP3 protein in the NLRP3/Caspase1/IL-1β pathway. The present study, together with our previous findings [29], suggests that Lg-induced neuronal protection is beneficial throughout the entire process of cerebral infarction. Therefore, Lg may be a promising drug for the treatment of ischemic stroke.

Supplementary Information The online version contains supplementary material available at https://doi.org/10.1007/s11064-022-03574-4.

Funding This work was generously supported by grants from the National Natural Science Foundation of China (Grant No. 81974184) and the Key Project of Medical Science Research in Hebei Province 2021 (Grant No. 20211706).

Data Availability Enquiries about data availability should be directed to the authors.

Declarations

Conflict of interest The authors declare no competing interest.

References

1. Benjamin EJ, Virani SS, Callaway CW, Chamberlain AM, Chang AR, Cheng S, Chiuve SE, Cushman M, Delling FN, Deo R, de Ferranti SD (2018) Correction to: heart disease and stroke statistics-2018 update: a report from the American Heart Association. Circulation 137:e493
2. Virani SS, Alonso A, Benjamin EJ, Bittencourt MS, Callaway CW, Carson AP, Chamberlain AM, Chang AR, Cheng S, Delling FN, Djousse L, Elkind MSV, Ferguson JF, Fornage M, Khan SS, Kissela BM, Knutson KL, Kwan TW, Lackland DT, Lewis TT, Lichtman JH, Longenecker CT, Loop MS, Lutsey PL, Martin SS, Matsushita K, Moran AE, Mussolino ME, Perak AM, Rosamond WD, Roth GA, Sampson UKA, Satou GM, Schroeder EB, Shah SH, Shay CM, Spartano NL, Stokes A, Tirschwell DL, VanWagner LB, Tsao CW, American Heart Association Council on E, Prevention Statistics C, Stroke Statistics S (2020) Heart disease and stroke statistics-2020 update: a report from the American Heart Association. Circulation 141:e139–e596
3. Zou Z, Cini K, Dong B, Ma Y, Ma J, Burgner DP, Patton GC (2020) Time trends in cardiovascular disease mortality across the BRICS: an age-period-cohort analysis of key nations with emerging economies using the global burden of disease study 2017. Circulation 141:790–799

4. Jahan R, Saver JL, Schwamm LH, Fonarow GC, Liang L, Matsouaka RA, Xian Y, Holmes DN, Peterson ED, Yavagal D, Smith EE (2019) Association between time to treatment with endovascular reperfusion therapy and outcomes in patients with acute ischemic stroke treated in clinical practice. JAMA 322:252–263
5. Shi J, Gao W, Shao F (2017) Pyroptosis: gasdermin-mediated programmed necrotic cell death. Trends Biochem Sci 42:245–254
6. Frank D, Vince JE (2019) Pyroptosis versus necroptosis: similarities, differences, and crosstalk. Cell Death Differ 26:99–114
7. Humphries F, Shmuel-Galia L, Ketelut-Carneiro N, Li S, Wang B, Nemmara VV, Wilson R, Jiang Z, Khalighinejad F, Muneeruddin K, Shaffer SA, Dutta R, Ionete C, Pesiridis S, Yang S, Thompson PR, Fitzgerald KA (2020) Succination inactivates gasdermin D and blocks pyroptosis. Science 369:1633–1637
8. Chen X, He WT, Hu L, Li J, Fang Y, Wang X, Xu X, Wang Z, Huang K, Han J (2016) Pyroptosis is driven by non-selective gasdermin-D pore and its morphology is different from MLKL channel-mediated necroptosis. Cell Res 26:1007–1020
9. Tu XK, Chen Q, Chen S, Huang B, Ren BG, Shi SS (2021) GLP-1R agonist liraglutide attenuates inflammatory reaction and neuronal apoptosis and reduces early brain injury after subarachnoid hemorrhage in rats. Inflammation 44:397–406
10. Bianchi M, D'Oria V, Braghini MR, Petrini S, Manco M (2019) Liraglutide treatment ameliorates neurotoxicity induced by stable silencing of Pin1. Int J Mol Sci 20:5064
11. Basalay MV, Davidson SM, Yellon DM (2019) Neuroprotection in rats following ischaemia-reperfusion injury by GLP-1 analogues-liraglutide and semaglutide. Cardiovasc Drugs Ther 33:661–667
12. Liu S, Jin Z, Zhang Y, Rong S, He W, Sun K, Wan D, Huo J, Xiao L, Li X, Ding N, Wang F, Sun T (2020) The glucagon-like peptide-1 analogue liraglutide reduces seizures susceptibility, cognition dysfunction and neuronal apoptosis in a mouse model of dravet syndrome. Front Pharmacol 11:136
13. Verma S, Bain SC, Buse JB, Idorn T, Rasmussen S, Orsted DD, Nauck MA (2019) Occurence of first and recurrent major adverse cardiovascular events with liraglutide treatment among patients with type 2 diabetes and high risk of cardiovascular events: a post hoc analysis of a randomized clinical trial. JAMA Cardiol 4:1214–1220
14. Yu X, Hao M, Liu Y, Ma X, Lin W, Xu Q, Zhou H, Shao N, Kuang H (2019) Liraglutide ameliorates non-alcoholic steatohepatitis by inhibiting NLRP3 inflammasome and pyroptosis activation via mitophagy. Eur J Pharmacol 864:172715
15. Percie du Sert N, Hurst V, Ahluwalia A, Alam S, Avey MT, Baker M, Browne WJ, Clark A, Cuthill IC, Dirnagl U, Emerson M, Garner P, Holgate ST, Howells DW, Karp NA, Lazic SE, Lidster K, MacCallum CJ, Macleod M, Pearl EJ, Petersen OH, Rawle F, Reynolds P, Rooney K, Sena ES, Silberberg SD, Steckler T, Wurbel H (2020) The ARRIVE guidelines 2.0: updated guidelines for reporting animal research. BMJ Open Sci 4:e100115
16. Pena-Philippides JC, Caballero-Garrido E, Lordkipanidze T, Roitbak T (2016) In vivo inhibition of miR-155 significantly alters post-stroke inflammatory response. J Neuroinflammation 13:287
17. Espinosa A, Meneses G, Chavarria A, Mancilla R, Pedraza-Chaverri J, Fleury A, Barcena B, Perez-Osorio IN, Besedovsky H, Arauz A, Fragoso G, Sciutto E (2020) Intranasal dexamethasone reduces mortality and brain damage in a mouse experimental ischemic stroke model. Neurotherapeutics 17:1907–1918
18. Xue J, Zhang X, Zhang C, Kang N, Liu X, Yu J, Zhang N, Wang H, Zhang L, Chen R, Cui L, Wang L, Wang X (2016) Protective effect of Naoxintong against cerebral ischemia reperfusion injury in mice. J Ethnopharmacol 182:181–189
19. Cui HY, Zhang XJ, Yang Y, Zhang C, Zhu CH, Miao JY, Chen R (2018) Rosmarinic acid elicits neuroprotection in ischemic stroke via Nrf2 and heme oxygenase 1 signaling. Neural Regen Res 13:2119–2128
20. Liu Y, Xue X, Zhang H, Che X, Luo J, Wang P, Xu J, Xing Z, Yuan L, Liu Y, Fu X, Su D, Sun S, Zhang H, Wu C, Yang J (2019) Neuronal-targeted TFEB rescues dysfunction of the autophagy-lysosomal pathway and alleviates ischemic injury in permanent cerebral ischemia. Autophagy 15:493–509
21. Gao C, Qian Y, Huang J, Wang D, Su W, Wang P, Guo L, Quan W, An S, Zhang J, Jiang R (2017) A three-day consecutive fingolimod administration improves neurological functions and modulates multiple immune responses of CCI mice. Mol Neurobiol 54:8348–8360
22. Liu XY, Hwang E, Park B, Xiao YK, Yi TH (2019) Photoprotective and anti-inflammatory properties of vina-ginsenoside R7 ameliorate ultraviolet B-induced photodamage in normal human dermal fibroblasts. Appl Biochem Biotechnol 189:729–744
23. Weise G, Posel C, Moller K, Kranz A, Didwischus N, Boltze J, Wagner DC (2017) High-dosage granulocyte colony stimulating factor treatment alters monocyte trafficking to the brain after experimental stroke. Brain Behav Immun 60:15–26
24. Chen J, Zhang X, Liu X, Zhang C, Shang W, Xue J, Chen R, Xing Y, Song D, Xu R (2019) Ginsenoside Rg1 promotes cerebral angiogenesis via the PI3K/Akt/mTOR signaling pathway in ischemic mice. Eur J Pharmacol 856:172418
25. Song D, Zhang X, Chen J, Liu X, Xue J, Zhang L, Lan X (2019) Wnt canonical pathway activator TWS119 drives microglial anti-inflammatory activation and facilitates neurological recovery following experimental stroke. J Neuroinflammation 16:256
26. Zhang N, Zhang X, Liu X, Wang H, Xue J, Yu J, Kang N, Wang X (2014) Chrysophanol inhibits NALP3 inflammasome activation and ameliorates cerebral ischemia/reperfusion in mice. Mediators Inflamm 2014:370530
27. Poh L, Kang SW, Baik SH, Ng GYQ, She DT, Balaganapathy P, Dheen ST, Magnus T, Gelderblom M, Sobey CG, Koo EH, Fann DY, Arumugam TV (2019) Evidence that NLRC4 inflammasome mediates apoptotic and pyroptotic microglial death following ischemic stroke. Brain Behav Immun 75:34–47
28. Madsen TE, Long DL, Carson AP, Howard G, Kleindorfer DO, Furie KL, Manson JE, Liu S, Howard VJ (2021) Sex and race differences in the risk of ischemic stroke associated with fasting blood glucose in REGARDS. Neurology 97:e684–e694
29. Chen Y, Zhang X, He J, Xie Y, Yang Y (2018) Delayed administration of the glucagon-like peptide 1 analog liraglutide promoting angiogenesis after focal cerebral ischemia in mice. J Stroke Cerebrovasc Dis 27:1318–1325
30. Sato K, Kameda M, Yasuhara T, Agari T, Baba T, Wang F, Shinko A, Wakamori T, Toyoshima A, Takeuchi H, Sasaki T, Sasada S, Kondo A, Borlongan CV, Matsumae M, Date I (2013) Neuroprotective effects of liraglutide for stroke model of rats. Int J Mol Sci 14:21513–21524
31. Zhang L, Li C, Zhu Q, Li N, Zhou H (2019) Liraglutide, a glucagon-like peptide-1 analog, inhibits high glucose-induced oxidative stress and apoptosis in neonatal rat cardiomyocytes. Exp Ther Med 17:3734–3740
32. Hernandez C, Bogdanov P, Corraliza L, Garcia-Ramirez M, Sola-Adell C, Arranz JA, Arroba AI, Valverde AM, Simo R (2016) Topical administration of GLP-1 receptor agonists prevents retinal neurodegeneration in experimental diabetes. Diabetes 65:172–187
33. Gejl M, Brock B, Egefjord L, Vang K, Rungby J, Gjedde A (2017) Blood–brain glucose transfer in Alzheimer's disease: effect of GLP-1 analog treatment. Sci Rep 7:17490
34. Geloneze B, de Lima-Junior JC, Velloso LA (2017) Glucagon-like peptide-1 receptor agonists (GLP-1RAs) in the brain-adipocyte axis. Drugs 77:493–503
35. Bizino MB, Jazet IM, Westenberg JJM, van Eyk HJ, Paiman EHM, Smit JWA, Lamb HJ (2019) Effect of liraglutide on cardiac function in patients with type 2 diabetes mellitus: randomized placebo-controlled trial. Cardiovasc Diabetol 18:55

36. Wicinski M, Socha M, Malinowski B, Wodkiewicz E, Walczak M, Gorski K, Slupski M, Pawlak-Osinska K (2019) Liraglutide and its neuroprotective properties-focus on possible biochemical mechanisms in Alzheimer's disease and cerebral ischemic events. Int J Mol Sci 20:1050
37. Athauda D, Foltynie T (2016) The glucagon-like peptide 1 (GLP) receptor as a therapeutic target in Parkinson's disease: mechanisms of action. Drug Discov Today 21:802–818
38. McKenzie BA, Mamik MK, Saito LB, Boghozian R, Monaco MC, Major EO, Lu JQ, Branton WG, Power C (2018) Caspase1 inhibition prevents glial inflammasome activation and pyroptosis in models of multiple sclerosis. Proc Natl Acad Sci USA 115:E6065–E6074
39. Holubova M, Hruba L, Popelova A, Bencze M, Prazienkova V, Gengler S, Kratochvilova H, Haluzik M, Zelezna B, Kunes J, Holscher C, Maletinska L (2019) Liraglutide and a lipidized analog of prolactin-releasing peptide show neuroprotective effects in a mouse model of beta-amyloid pathology. Neuropharmacology 144:377–387
40. Farr OM, Upadhyay J, Rutagengwa C, DiPrisco B, Ranta Z, Adra A, Bapatla N, Douglas VP, Douglas KAA, Nolen-Doerr E, Mathew H, Mantzoros CS (2019) Longer-term liraglutide administration at the highest dose approved for obesity increases reward-related orbitofrontal cortex activation in response to food cues: Implications for plateauing weight loss in response to anti-obesity therapies. Diabetes Obes Metab 21:2459–2464
41. Bai XJ, Hao JT, Zheng RH, Yan CP, Wang J, Yang CH, Zhang WF, Zhao ZQ (2021) Glucagon-like peptide-1 analog liraglutide attenuates pressure-overload induced cardiac hypertrophy and apoptosis through activating ATP sensitive potassium channels. Cardiovasc Drugs Ther 35:87–101
42. Yang X, Ma X, Don O, Song Y, Chen X, Liu J, Qu J, Feng Y (2020) Mesenchymal stem cells combined with liraglutide relieve acute lung injury through apoptotic signaling restrained by PKA/beta-catenin. Stem Cell Res Ther 11:182
43. Rakipovski G, Rolin B, Nohr J, Klewe I, Frederiksen KS, Augustin R, Hecksher-Sorensen J, Ingvorsen C, Polex-Wolf J, Knudsen LB (2018) The GLP-1 analogs liraglutide and semaglutide reduce atherosclerosis in ApoE(-/-) and LDLr(-/-) mice by a mechanism that includes inflammatory pathways. JACC Basic Transl Sci 3:844–857
44. Eftekhari S, Montazeri H, Tarighi P (2020) Synergistic anti-tumor effects of Liraglutide, a glucagon-like peptide-1 receptor agonist, along with Docetaxel on LNCaP prostate cancer cell line. Eur J Pharmacol 878:173102
45. Helmstadter J, Keppeler K, Aust F, Kuster L, Frenis K, Filippou K, Vujacic-Mirski K, Tsohataridis S, Kalinovic S, Kroller-Schon S, Oelze M, Bosmann M, Munzel T, Daiber A, Steven S (2021) GLP-1 analog liraglutide improves vascular function in polymicrobial sepsis by reduction of oxidative stress and inflammation. Antioxidants (Basel) 10:1175
46. Nizari S, Basalay M, Chapman P, Korte N, Korsak A, Christie IN, Theparambil SM, Davidson SM, Reimann F, Trapp S, Yellon DM, Gourine AV (2021) Glucagon-like peptide-1 (GLP-1) receptor activation dilates cerebral arterioles, increases cerebral blood flow, and mediates remote (pre)conditioning neuroprotection against ischaemic stroke. Basic Res Cardiol 116:32
47. Hattori Y, Jojima T, Tomizawa A, Satoh H, Hattori S, Kasai K, Hayashi T (2010) A glucagon-like peptide-1 (GLP-1) analogue, liraglutide, upregulates nitric oxide production and exerts anti-inflammatory action in endothelial cells. Diabetologia 53:2256–2263
48. Bai B, Li D, Xue G, Feng P, Wang M, Han Y, Wang Y, Holscher C (2021) The novel GLP-1/GIP dual agonist DA3-CH is more effective than liraglutide in reducing endoplasmic reticulum stress in diabetic rats with cerebral ischemia-reperfusion injury. Nutr Metab Cardiovasc Dis 31:333–343
49. Briyal S, Shah S, Gulati A (2014) Neuroprotective and anti-apoptotic effects of liraglutide in the rat brain following focal cerebral ischemia. Neuroscience 281:269–281
50. Babic I, Sellers D, Else PL, Nealon J, Osborne AL, Pai N, Weston-Green K (2021) Effect of liraglutide on neural and peripheral markers of metabolic function during antipsychotic treatment in rats. J Psychopharmacol 35:284–302
51. He W, Wang H, Zhao C, Tian X, Li L, Wang H (2020) Role of liraglutide in brain repair promotion through Sirt1-mediated mitochondrial improvement in stroke. J Cell Physiol 235:2986–3001
52. Basalay MV, Davidson SM, Yellon DM (2020) Can glucagon-like peptide-1 (GLP-1) analogues make neuroprotection a reality? Neural Regen Res 15:1852–1853
53. Miao EA, Rajan JV, Aderem A (2011) Caspase1-induced pyroptotic cell death. Immunol Rev 243:206–214
54. Zhang D, Qian J, Zhang P, Li H, Shen H, Li X, Chen G (2019) 4.163 3) Gasdermin D serves as a key executioner of pyroptosis in experimental cerebral ischemia and reperfusion model both in vivo and in vitro. J Neurosci Res 97:645–660
55. Yan J, Xu W, Lenahan C, Huang L, Wen J, Li G, Hu X, Zheng W, Zhang JH, Tang J (2021) CCR5 activation promotes NLRP1-dependent neuronal pyroptosis via CCR5/PKA/CREB pathway after intracerebral hemorrhage. Stroke 52:4021–4032
56. Xie B, Liu T, Chen S, Zhang Y, He D, Shao Q, Zhang Z, Wang C (2021) Combination of DNA demethylation and chemotherapy to trigger cell pyroptosis for inhalation treatment of lung cancer. Nanoscale 13:18608–18615
57. An H, Heo JS, Kim P, Lian Z, Lee S, Park J, Hong E, Pang K, Park Y, Ooshima A, Lee J, Son M, Park H, Wu Z, Park KS, Kim SJ, Bae I, Yang KM (2021) Tetraarsenic hexoxide enhances generation of mitochondrial ROS to promote pyroptosis by inducing the activation of caspase-3/GSDME in triple-negative breast cancer cells. Cell Death Dis 12:159
58. van Hout GP, Bosch L, Ellenbroek GH, de Haan JJ, van Solinge WW, Cooper MA, Arslan F, de Jager SC, Robertson AA, Pasterkamp G, Hoefer IE (2017) The selective NLRP3-inflammasome inhibitor MCC950 reduces infarct size and preserves cardiac function in a pig model of myocardial infarction. Eur Heart J 38:828–836
59. Wang T, Nowrangi D, Yu L, Lu T, Tang J, Han B, Ding Y, Fu F, Zhang JH (2018) Activation of dopamine D1 receptor decreased NLRP3-mediated inflammation in intracerebral hemorrhage mice. J Neuroinflammation 15:2
60. He Y, Hara H, Nunez G (2016) Mechanism and regulation of NLRP3 inflammasome activation. Trends Biochem Sci 41:1012–1021
61. Broz P, Dixit VM (2016) Inflammasomes: mechanism of assembly, regulation and signalling. Nat Rev Immunol 16:407–420
62. Feigin V, Lawes C, Bennett D, Anderson C (2003) Stroke epidemiology: a review of population-based studies of incidence, prevalence, and case-fatality in the late 20th century. Lancet Neurol 2:43–53
63. Kleindorfer DO, Towfighi A, Chaturvedi S, Cockroft KM, Gutierrez J, Lombardi-Hill D, Kamel H, Kernan WN, Kittner SJ, Leira EC, Lennon O, Meschia JF, Nguyen TN, Pollak PM, Santangeli P, Sharrief AZ, Smith SC Jr, Turan TN, Williams LS (2021) 2021 Guideline for the prevention of stroke in patients with stroke and transient ischemic attack: a guideline from the American Heart Association/American Stroke Association. Stroke 52:e364–e467